ICM11

Fatigue behavior of notched Ti-6Al-4V in air and corrosive environment

S. Baragetti[a,b,]*, S. Cavalleri[b] and F. Tordini[a]

[a]*Department of Design and Technology, University of Bergamo, Viale Marconi 5, Dalmine 24044, Italy*
[b]*GITT - Centre on Innovation Management and Technology Transfer, University of Bergamo, Via Salvecchio 19, Bergamo 24129, Italy*

Abstract

The broad use of titanium alloys in naval, automotive and aerospace applications expects the current research to shed light on the fatigue behavior of these materials in corrosive media and notched condition. In this respect, the fatigue behavior in air and NaCl solution of notched Ti-6Al-4V flat dogbone samples was investigated. A step-loading method was used to generate data points on fatigue limit stress vs. K_t diagrams for a constant life of 200,000 load cycles at R = 0.1. Fracture surfaces were observed using stereoscopic microscope.

Keywords: Ti-6Al-4V; Fatigue; V-notch; Environmental effect; Step-loading technique

1. Introduction

Ti-6Al-4V titanium alloy is widely used for advanced military and civil aerospace and naval applications because of its good corrosion resistance and high strength-to-mass ratio. The current research is then expected to study the fatigue behaviour of this alloy more and more thoroughly. The fatigue resistance of smooth and notched Ti-6Al-4V has extensively been investigated in standard laboratory conditions [1-5]. Nevertheless, a deeper understanding of the fatigue strength of Ti-6Al-4V components while operating in corrosive media and/or after foreign object damage (e.g. aircraft or offshore applications) is urged to be gained to prevent dramatic failures due to environment-assisted fatigue or notch-induced fatigue crack growth [6,7]. In fact, studies on the fatigue behavior under aggressive environment of notched Ti-6Al-4V at high K_t are missing in literature. In this work, axial fatigue tests (R = 0.1) in air and recirculated 3.5 wt.% NaCl solution were carried out on notched flat Ti-6Al-4V samples at stress concentration factors up to more than 13. V-notches were machined within the gage length to have K_t between 2.55 and 13.34 with the minimum sample cross section and notch depth held constant. A step-loading technique [4,5,8] was used to generate data points on linear and logarithmic fatigue limit vs. K_t diagrams [9,10] for a constant fatigue life of 2×10^5 load cycles. This representation allowed highlighting the effects of the aggressive environment in comparison with the laboratory air condition. A selection of fracture surfaces was observed using stereoscopic

---

* Corresponding author. Tel.: +39-035-2052382; fax: +39-035-2052310.
E-mail address: sergio.baragetti@unibg.it.

microscope.

Nomenclature

N_f number of cycles to failure in the final loading block

$\sigma_{final,max}$ maximum applied stress on minimum cross section in the loading block when failure occurred (MPa)

$\sigma_{prior,max}$ maximum applied stress on minimum cross section in the loading block prior to that of failure (MPa)

$\sigma_{FL,max}$ interpolated fatigue limit (maximum stress over the fatigue cycle) at 2×10^5 cycles (MPa)

$\sigma_{alt,lim}$ limiting alternating stress component at 2×10^5 cycles (MPa)

2. Experimental techniques

This study was carried out on Ti-6Al-4V titanium alloy with the following average chemical composition (wt.%): 5.97 Al, 4.07 V, 0.20 Fe, 0.1885 O, 0.003 C and Ti bal. The geometry of the fatigue dogbone V-notched flat samples is shown in Fig. 1. They were machined from hot rolled plate so as to have the notch axis parallel to the rolling direction (L-direction) of the parent Ti-6Al-4V plate. A solution treatment at 925°C (1 h) and vacuum annealing at 700°C (2 h) for stabilization was carried out prior to the machining operations. The notches were formed by milling at very low cutting speed to limit the residual stresses, then by electrical discharge machining (EDM) to obtain the precise values of the following notch root radii (ρ): 0.06, 0.26, 1.50 and 2.50 mm. The associated stress concentration factors K_t determined by finite element modelling were, respectively: 13.34, 6.63, 3.10 and 2.55. All the samples were finally stress relieved at 700°C in vacuum for 1 h before being tested under fatigue. The static strength along the transversal direction (LT-direction), which coincided with that of load application, after the solution and overaging treatment (STOA) was determined with tensile tests (INSTRON 1273).
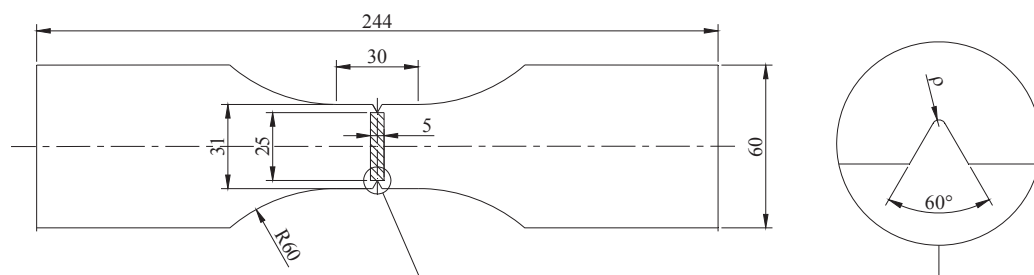

Fig. 1. Fatigue sample geometry (dimensions in mm).

Axial fatigue tests (R = 0.1) were carried out with a computer-controlled universal testing machine (BRT T1000, Italy) at a frequency of 10 Hz with an upper limit of 2×10^5 cycles in laboratory air and recirculated 3.5 wt.% NaCl solution. The limiting maximum stress was calculated by means of a step-loading technique [4,5,8], which allows rapid determination of a reliable value [8] of the fatigue limit at the desired number cycles by cycling only a sample under stepwise incremental loads. By assuming that the alternating stress component is half of the stress range, the limiting alternating stress $\sigma_{alt,lim}$ was plotted vs. K_t on both linear and Log scale diagrams. Each sample was tested at an initial stress level presumed to be lower than the fatigue limit according to literature data [11,12] and, provided that the sample had not failed after the first 2×10^5 load cycles, it was cycled again for another block of 2×10^5 cycles at a stress level increased by a small percentage of 5%. This was repeated until sample failure. Small acetate strips were used to take replicas every 5×10^3-10^4 cycles to detect the presence of possible propagating cracks at the notch roots as early as possible and to allow their growth to be monitored by optical image (Leica DFC290) analysis. The fatigue limit stress $\sigma_{FL,max}$ at the complete fracture was determined by interpolating between the maximum stress of the last two loading blocks according to the following formula where the stresses are the nominal ones over the minimum sample cross section without the presence of the notch:

$$\sigma_{\text{FL,max}} = \sigma_{\text{prior,max}} + \frac{N_{\text{f}}}{2 \times 10^5} \left(\sigma_{\text{final,max}} - \sigma_{\text{prior,max}} \right)$$

Coaxing, which consists in fatigue strength increase when a component is cycled below its fatigue limit, may potentially affect the reliability of the results. However, this phenomenon is typical of ferrous materials [10,13] and the step-loading method has already applied with good results to Ti-6Al-4V [4,5,8]. Some fracture surfaces were examined using stereoscopic microscope (Nikon SMZ800) to have an overview of the main features of the fatigue crack propagation process.
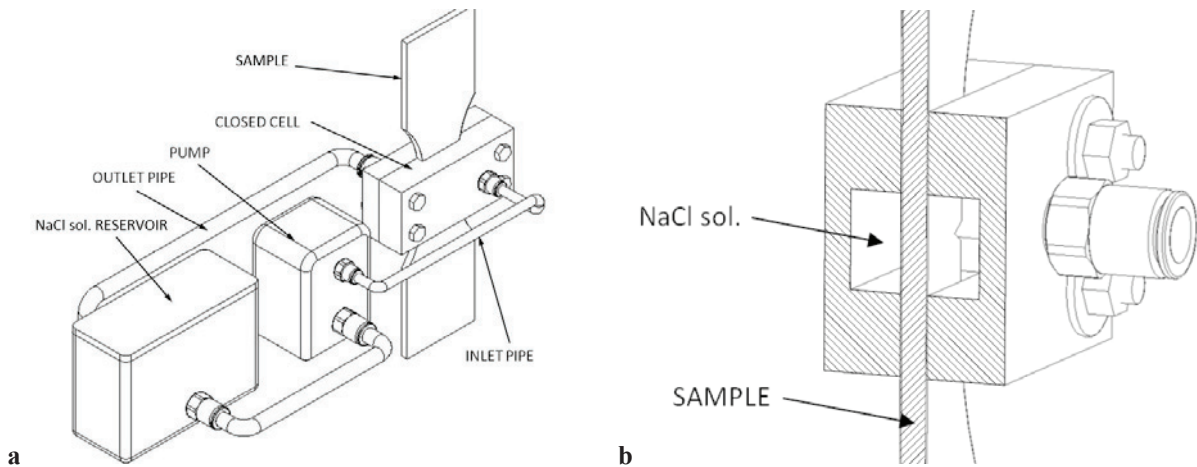

Fig. 2. (a) Sketch of the equipment used for the tests in NaCl solution and (b) detail of the closed cell (cross sectioned).

A watertight cell with a suitable recirculation system was assembled for the tests in NaCl solution so that the sample notch area was completely submerged in the corrosive medium which was continuously pumped through the recirculation circuit. Figs. 2a and 2b show sketches of the system and a detail of the cell respectively. The system was composed of the closed cell equipped with two corrosion-resistant threaded rapid tubing connections, a solution reservoir, a pump and suitable piping connections. The cell consisted of two Plexiglas shells joined by bolting and sealed with sealing filler. The shells could be easily separated and joined together again whenever surface replicas had to be taken during the fatigue tests. In order to prevent the internal pressure from rising during the tests, the diameter of the outlet pipe of the cell was greater than the diameter of the inlet pipe.

3. Results and discussion

The tensile and yield strength along the LT-direction of Ti-6Al-4V after STOA were, respectively, 990 and 945 MPa. The Young's modulus was 110,000 MPa. Figs. 3a and 3b show the crack lengths determined with the surface replicas plotted vs. the number of cycles spent in propagation for samples tested in air and NaCl solution respectively. Based on the experimental evidence, very high crack growth rates were observed in both the test environments. In all the tests the complete fracture occurred after a relatively low number of cycles after having detected the propagating crack. Compared with the tests in air, crack growth rate was higher in NaCl solution at all the stress concentration factors. Furthermore, this environment-assisted accelerated crack growth was more evident at low K_t, where samples failed in a few thousand of cycles. Consistently with the lower applied load levels, crack growth rates at high K_t were lower than they were at low K_t in both the environments.

Figs. 4a and 4b show the experimental results of the tests in laboratory air and NaCl solution converted into data points on, respectively, $\sigma_{\text{alt,lim}}$ vs. K_t linear and Log scale diagrams for a constant life of 2×10^5 load cycles. Compared with the tests in air, a significant reduction – down to -28% – in the limiting stress took place in NaCl solution for the samples with K_t lower than 6.63. Unpredictably, a remarkable fatigue limit improvement of +19% was seen at $K_t = 6.63$. Beyond the intermediate K_t range the NaCl solution was again detrimental to the fatigue resistance of notched Ti-6Al-4V, although its effect was less important than at low K_t. Therefore, such a

discontinuity in the trend of data points suggests that a critical K_t range between 3.10 and 13.34, where the fatigue behaviour of the samples tested in NaCl solution becomes better than that observed in air, could exist. A tentative explanation for the improved fatigue behaviour of the samples with $K_t = 6.63$ may be that air pockets could have remained trapped at the notch roots with radius equal to 0.26 mm preventing the notch root area from getting into contact with the NaCl solution. Anyhow, the lower detrimental effect of the saline solution within the intermediate K_t range needs to be verified with further tests at K_t values within a range around 6.63. Furthermore, a tendency of the limiting alternating stress to approach asymptotically to a lower limit as the stress concentration factor rises can be seen regardless of the test environment.
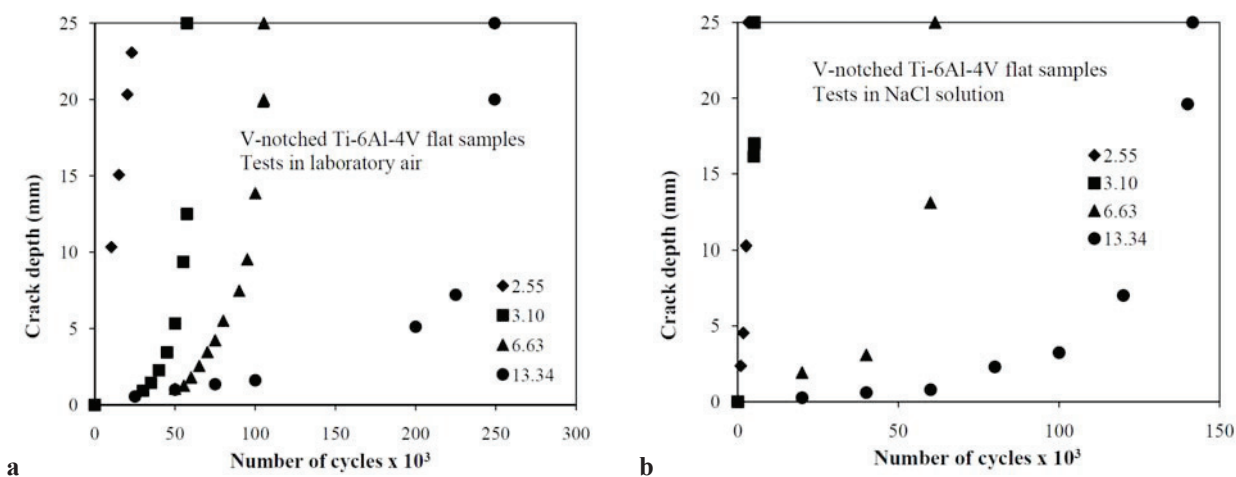

Fig. 3. Detected crack depth vs. Number of cycles since initiation occurrence in (a) laboratory air and (b) NaCl solution.

The rearrangement of the data points on a Log-Log diagram (Fig. 4b) allows drawing a bilinear interpolating curve averaging the results of both the test environments. After the first stage of decrease at low K_t, a threshold stress concentration factor between 6 and 7, beyond which the limiting alternating stress seems not to change significantly regardless of the test environment, could be assumed. This, as well as the fatigue behavior in NaCl solution at intermediate K_t values, is intended to be investigated with further tests.
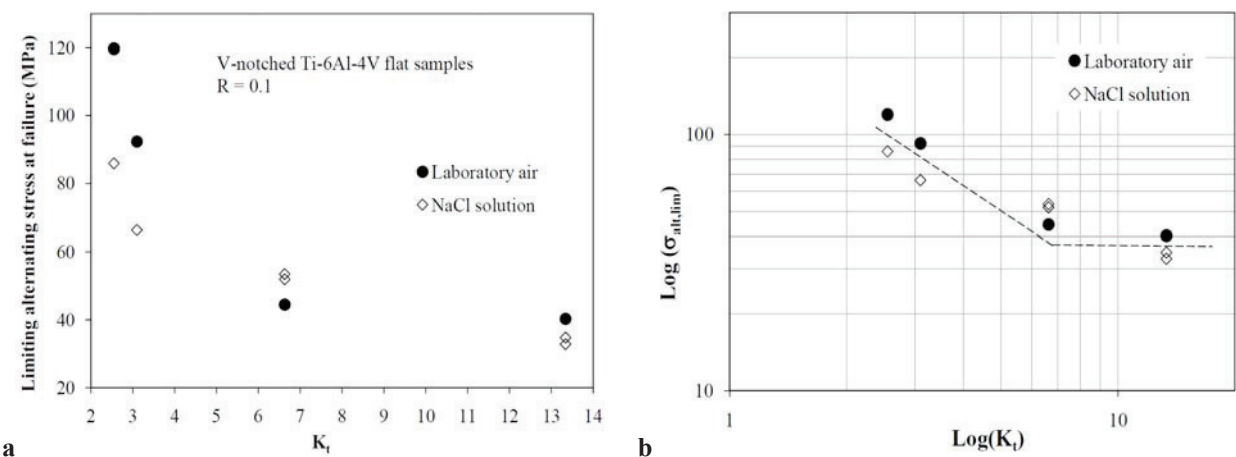

Fig. 4. Limiting alternating stress vs. K_t (a) linear and (b) Log scale diagrams.

Some micrographs of the fracture surfaces were taken using stereoscopic microscope to capture evident features of the fatigue crack propagation process. Fig. 5a shows an overview of the stable propagation area of the fracture surface of sample with $K_t = 3.10$ tested in NaCl solution. Typical beach marks, which could be associated with the

arrest and load increase operations between steps, can be seen in the middle, whereas the boundary of the final overload area is visible on the right. This boundary separates the smoother sub-critical (left) side from the unstable crack propagation region. Single side crack initiation occurred, as the whole final plastic deformation is localized at the notch root area where no fatigue damage took place (right side of Fig. 5b). A detail of this region is shown in Fig. 5c, which magnifies the plasticized area behind the notch root.
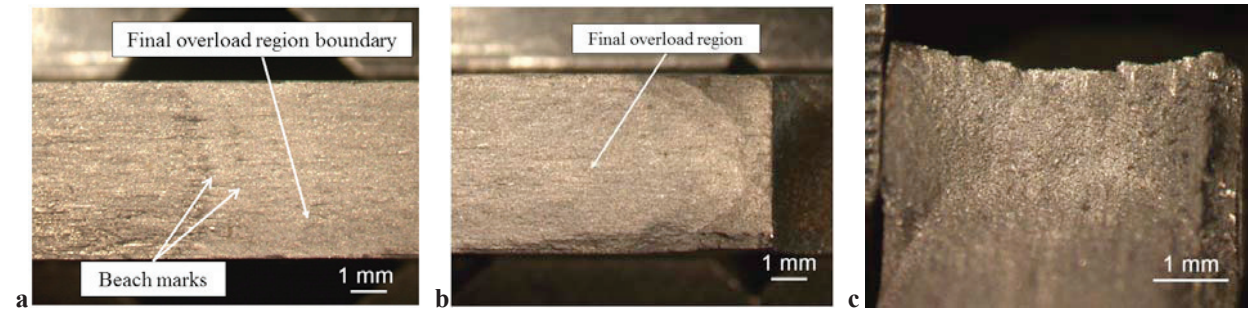

Fig. 5. Fracture surface of sample with $K_t = 3.10$ tested in NaCl solution: (a) overview of the stable propagation region, (b) final overload area and detail (c) of the plasticized area behind the notch root.

The fracture surface of sample with $K_t = 13.34$ cycled in air is shown in Fig. 6. An overview of the crack initiation area behind the notch root characterized by higher crack growth rate is illustrated in Fig 6a. Evident beach marks emanating from the left notch root are visible. In this sample, fatigue crack propagation occurred from both the notch roots, as the presence of a small stable propagation area behind the right notch root was observed (Fig. 6b). Two beach marks emanating from the notch root and a small region of large deformation associated with the final overload failure are shown in Fig 6b.
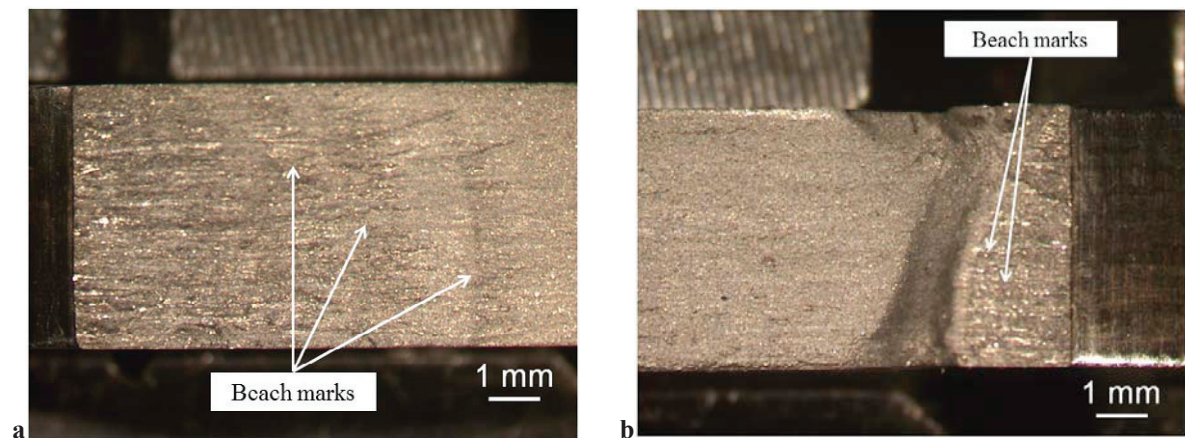

Fig. 6. Fracture surface of sample with $K_t = 13.34$ tested in air: (a) stable propagation region characterized by higher crack growth rate and (b) final overload region where a secondary stable propagation area can be seen.

4. Conclusions

Axial fatigue tests (R = 0.1) in air and recirculated 3.5 wt.% NaCl solution were carried out on V-notched flat dogbone Ti-6Al-4V samples with stress concentration factors of 2.55, 3.10, 6.63 and 13.34. A step-loading technique was implemented to determine the fatigue limit for a constant fatigue life of 2×10^5 load cycles. Based on the experimental results, the following points are underlined:

- High crack growth rates were observed regardless of K_t and test environment
- Crack growth rates in NaCl solution were higher than they were in air at all the K_t investigated
- A fatigue limit reduction down to -28% was found for the samples tested in NaCl solution at K_t lower than 6.63
- A discontinuity in the fatigue limit trend was found at $K_t = 6.63$, where the behaviour of the notched samples

S. Baragetti et al. / Procedia Engineering 10 (2011) 2435–2440

tested in NaCl solution was better than that of the sample tested in air
- A threshold stress concentration factor, beyond which the fatigue limit seemed not to change regardless of the test environment, was assumed between 6 and 7

Acknowledgements

References

[1] Lanning DB, Haritos GK, Nicholas T. Influence of stress state on high cycle fatigue of notched Ti-6Al-4V specimens. *Int J Fat* 1999; 21:S87–95.

[2] Lanning DB, Haritos GK, Nicholas T, Maxwell DC. Low-cycle fatigue/high-cycle fatigue interactions in notched Ti–6Al–4V. *Fatigue Fract Engng Mater Struct* 2001; 24:565–77.

[3] Naika RA, Lanning DB, Nicholas T, Kallmeyer AR. A critical plane gradient approach for the prediction of notched HCF life. *Int J Fat* 2005; 27:481–49.

[4] Lanning DB, Nicholas T, Palazotto A. The effect of notch geometry on critical distance high cycle fatigue predictions. *Int J Fat* 2005; 27:1623–27.

[5] Lanning DB, Nicholas T, Haritos GK. On the use of critical distance theories for the prediction of the high cycle fatigue limit stress in notched Ti–6Al–4V. *Int J Fat* 2005; 27:45–57.

[6] Kushan MC, Diltemiz SF, Sackesen İ. Failure analysis of an aircraft propeller. *Eng Fail Anal* 2007; 14:1693–1700.

[7] Boyer R, Welsch G, Collings EW. Materials Properties Handbook: Titanium Alloys, ASM International, Materials Park, Ohio; 1994, p. 554–78.

[8] Nicholas T. Step loading for very high cycle fatigue. *Fatigue Fract Engng Struct* 2002; 25:861–9.

[9] Frost NE, Dugdale DS. Fatigue tests on notched mild steel plates with measurement of fatigue cracks. *J Mech Phys Solids* 1957; 5:182–92.

[10] Frost NE, Marsh KJ, Pook LP. Metal Fatigue, Clarendon Press, Oxford; 1974, p. 130–201.

[11] Lanning DB, Nicholas T, Palazotto A. HCF notch predictions based on weakest-link failure models. *Int J Fat* 2003; 25:835–41.

[12] Morrissey RJ, Nicholas T. Fatigue strength of Ti-6Al-4V at very long lives. *Int J Fat* 2005; 27:1608–12.

[13] Sinclair GM. An investigation of the coaxing effect in fatigue of metals. *Proc ASTM* 1952; 52:743–58.

[14] Silveira E, Atxaga G, Irisarri AM. Failure analysis of two sets of aircraft blades. *Eng Fail Anal* 2010; 17:641–7.

[15] Chen X. Foreign object damage on the leading edge of a thin blade. *Mech Mater* 2005; 37:447–57.

[16] Ruschau J, Thompson SR, Nicholas T. High cycle fatigue limit stresses for airfoils subjected to foreign object damage. *Int J Fat* 2003; 25:955–62.